Tuning of an active photonic crystal cavity by an hybrid silica/silicon near-field probe

G. Le Gac[1,*], A. Rahmani[3], C. Seassal[1], E. Picard[2], E. Hadji[2], S. Callard[1,4]

[1] *Université de Lyon, Institut des Nanotechnologies de Lyon INL-UMR 5270, CNRS, Ecole Centrale de Lyon, 36 Avenue Guy de Collongue, F-69134 Ecully Cedex*
[2] *INAC /SP2M, LaboratoireSiNaPS, CEA Grenoble, 17 rue des martyrs, F-38054 Grenoble, France*
[3] *Department of Mathematical Science, University of Technology, Sydney, NSW 2007 Australia*
[4] *segolene.callard@ec-lyon.fr,*
**gaelle.le-gac@ec-lyon.fr*

Abstract: The influence of a near-field tip on the spectral characteristics of a resonant mode of an active photonic crystal micro-cavity was investigated. The wavelength shift of the mode was theoretically and experimentally demonstrated and evaluated as a function of the nature and the position of the tip above the cavity. Experiment showed that the shift induced is ten times higher with a Si-coated silica probe than with a bare silica tip: a shift until 2 nm was reached with Si-coated tip whereas the shift with bare silica tip is in the range of the tenth of nanometer, for wavelengths around 1,55 µm.

OCIS codes: (180.4243) Near-field microscopy ; (230.5298) Photonic crystals ; (130.3130) Integrated optics devices.

References and links

1. Y. Akahane, T. Asano, B.-S. Song, and S. Noda, "High-Q photonic nanocavity in a two-dimensional photonic crystal," Nature **425**(6961), 944–947 (2003).
2. M. Fujita, S. Takahashi, Y. Tanaka, T. Asano, and S. Noda, "Simultaneous inhibition and redistribution of spontaneous light emission in photonic crystals," Science **308**(5726), 1296–1298 (2005).
3. D. Englund, D. Fattal, E. Waks, G. Solomon, B. Zhang, T. Nakaoka, Y. Arakawa, Y. Yamamoto, and J. Vucković, "Controlling the spontaneous emission rate of single quantum dots in a two-dimensional photonic crystal," Phys. Rev. Lett. **95**(1), 013904 (2005).
4. K. Kounoike, M. Yamaguchi, M. Fujita, T. Asano, J. Nakanishi, and S. Noda, "Investigation of spontaneous emission from quantum dots embedded in two-dimensional photonic-crystal slab," Electron. Lett. **41**(25), 1402 (2005).
5. J. Vučković, and Y. Yamamoto, "Photonic crystal microcavities for cavity quantum electrodynamics with a single quantum dotl," Appl. Phys. Lett. **82**(15), 2374 (2003).
6. D. Gérard, L. Berguiga, F. de Fornel, L. Salomon, C. Seassal, X. Letartre, P. Rojo-Romeo, and P. Viktorovitch, "Near-field probing of active photonic-crystal structures," Opt. Lett. **27**(3), 173–175 (2002).
7. D.-J. Shin, S.-H. Kim, J.-K. Hwang, H.-Y. Ryu, H.-G. Park, D.-S. Song, and Y.-H. Lee, "Far- and near-field investigations on the lasing modes intwo-dimensional photonic crystal slab lasers," IEEE J. Quantum Electron. **38**(7), 857–866 (2002).
8. E. Flück, M. Hammer, A. M. Otter, J. P. Korterik, L. Kuipers, and N. F. van Hulst, "Amplitude and Phase Evolution of Optical Fields Inside Periodic Photonic Structures," J. Lightwave Technol. **21**(5), 1384–1393 (2003).
9. K. Okamoto, M. Loncar, T. Yoshie, A. Scherer, Y. Qiu, and P. Gogna, "Near-field scanning optical microscopy of photonic crystal nanocavities," Appl. Phys. Lett. **82**(11), 1676 (2003).
10. P. Kramper, M. Agio, C. M. Soukoulis, A. Birner, F. Müller, R. B. Wehrspohn, U. Gösele, and V. Sandoghdar, "Highly directional emission from photonic crystal waveguides of subwavelength width," Phys. Rev. Lett. **92**(11), 113903 (2004).
11. P. Kramper, M. Kafesaki, C. M. Soukoulis, A. Birner, F. Müller, U. Gösele, R. B. Wehrspohn, J. Mlynek, and V. Sandoghdar, "Near-field visualization of light confinement in a photonic crystal microresonator," Opt. Lett. **29**(2), 174–176 (2004).
12. N. Louvion, D. Gérard, J. Mouette, F. de Fornel, C. Seassal, X. Letartre, A. Rahmani, and S. Callard, "Local observation and spectroscopy of optical modes in an active photonic-crystal microcavity," Phys. Rev. Lett. **94**(11), 113907 (2005).
13. A. Faraon, and J. Vuckovic, "Local temperature control of photonic crystal devices via micron-scale electrical heaters," Appl. Phys. Lett. **95**(4), 043102 (2009).
14. A. Faraon, D. Englund, D. Bulla, B. Luther-Davies, B. J. Eggleton, N. Stoltz, P. Petroff, and J. Vuckovic, "Local Tuning of Photonic Crystal Cavities using Chalcogenide Glasses," Appl. Phys. Lett. **92**(4), 043123 (2008).

#116594 - $15.00 USD Received 2 Sep 2009; revised 9 Oct 2009; accepted 9 Oct 2009; published 11 Nov 2009

15. A. F. Koenderink, M. Kafesaki, B. C. Buchler, and V. Sandoghdar, "Controlling the resonance of a photonic crystal microcavity by a near-field probe," Phys. Rev. Lett. **95**(15), 153904 (2005).
16. A. F. Koenderink, R. Wüest, B. C. Buchler, S. Richter, P. Strasser, M. Kafesaki, A. Rogach, R. B. Wehrspohn, C. M. Soukoulis, D. Erni, F. Robin, H. Jackel, and V. Sandoghdar, "Near-field optics and control of photonic crystals," Photon. Nanostrut. **3**(2-3), 63–74 (2005).
17. I. Märki, M. Salt, and H. P. Herzig, "Tuning the resonance of a photonic crystal microcavity with an AFM probe," Opt. Express **14**(7), 2969–2978 (2006).
18. W. C. L. Hopman, K. O. van der Werf, A. J. Hollink, W. Bogaerts, V. Subramaniam, and R. M. de Ridder, "Nano-mechanical tuning and imaging of a photonic crystal micro-cavity resonance," Opt. Express **14**(19), 8745–8752 (2006).
19. S. Mujumdar, A. F. Koenderink, T. Sünner, B. C. Buchler, M. Kamp, A. Forchel, and V. Sandoghdar, "Near-field imaging and frequency tuning of a high-Q photonic crystal membrane microcavity," Opt. Express **15**(25), 17214–17220 (2007).
20. S. Mujumdar, A. F. Koenderink, R. Wüest, and V. Sandoghdar, "Nano-optomechanical characterization and manipulation of photonic crystals," IEEE J. Quantum Electron. **13**(2), 253–261 (2007).
21. L. Lalouat, B. Cluzel, P. Velha, E. Picard, D. Peyrade, J. P. Hugonin, P. Lalanne, E. Hadji, and F. de Fornel, "Near-field interactions between a subwavelength tip and a small-volume photonic-crystal nanocavity," Phys. Rev. B **76**(4), 041102 (2007).
22. B. Cluzell, L. Lalouat, P. Velha, E. Picard, D. Peyrade, J. C. Rodier, T. Charvolin, P. Lalanne, F. de Fornel, and E. Hadji, "A near-field actuated optical nanocavity," Opt. Express **16**(1), 279–286 (2008).
23. S.-H. Kim, G.-H. Kim, S.-K. Kim, H.-G. Park, Y.-H. Lee, and S.-B. Kim, "Characteristics of a stick waveguide resonator in a two-dimensional photonic crystal slab," J. Appl. Phys. **95**, 2 (2003).
24. Y.-S. Choi, M. T. Rakher, K. Henessy, S. Strauf, A. Badolato, P. M. Petroff, D. Bouwmeestern, and E. L. Lu, "Evolution of the onset of coherence in a family of photonic crystal nanolasers," Appl. Phys. Lett. **91**(3), 031108 (2007).
25. C. Monat, C. Seassal, X. Letartre, P. Regreny, P. Rojo Romeo, and P. Viktorovitch, M. Le Vassor d'Yerville, D. Cassagne, J. P. Albert, E. Jalaguier, S. Pocas, and B. Aspar, "InP-based two-dimensionnal photonic crystal on silicon: InP-plane Bloch mode laser," Appl. Phys. Lett. **81**, 5102 (2002).
26. C. Monat, C. Seassal, X. Letartre, P. Regreny, M. Gendry, P. Rojo Romeo, and P. Viktorovitch, M. Le Vassor d'Yerville, D. Cassagne, J. P. Albert, E. Jalaguier, S. Pocas, and B. Aspar, "Two-dimensional hexagonal-shaped microcavities formed in a two-dimensional photonic crystal on an InP membrane," J. Appl. Phys. **93**(1), 23 (2003).
27. N. Louvion, A. Rahmani, C. Seassal, S. Callard, D. Gérard, and F. de Fornel, "Near-field observation of subwavelength confinement of photoluminescence by a photonic crystal microcavity," Opt. Lett. **31**(14), 2160–2162 (2006).

1. Introduction

Two-dimensional photonic crystals (2D-PC) provide us with an unprecedented ability to control and confine photons. They are versatile building blocks for nanooptical architectures. In particular, PC slab structures, which rely on total internal reflection for the vertical optical confinement, and the photonic bandgap effect for the in-plane confinement, play an increasingly important role in nanophotonics. When combined with defect engineering, such structures can support localized modes with small mode volumes and large quality factors [1]. When coupled to a single emitter like a quantum dot, these PC structures can be used to enhance or inhibit the dynamics of the source [2–4], or as a source of nonclassical light [5]. The efficiency of the coupling between the emitter and the cavity depends both on the spectral matching and the spatial overlap between the cavity mode and the emitter. To address the issue of the optimal positioning of an emitter inside a cavity it is crucial to know the actual cavity mode profile on a small enough scale. For that purpose, near-field scanning optical microscopy (NSOM) has proved to be an invaluable tool as it gives us access to the mode profiles inside the cavity with a spatial resolution beyond what can be achieved with far-field techniques [6–12]. These studies showed that the near-field probing yields important information such as the local spectral response of a structure, or light intensity distribution inside a nanophotonic component. However, the potential of 2D-PC structures to foster new photonic devices would be greatly enhanced if their optical properties could be modified after fabrication. In particular, for active structures, the ability to post-tune, *in a reversible way,* a cavity to match the emission or absorption line of an emitter is of great interest. With devices operating at cryogenic temperatures the post-tuning can be achieved by varying the temperature of the PC device, using for instance electrical contacts [13]. Another approach consists in using the nonlinearity of another material to tune the cavity mode [14]. However, these techniques are not ideal for devices operating at room-temperature, or to achieve a local

#116594 - $15.00 USD Received 2 Sep 2009; revised 9 Oct 2009; accepted 9 Oct 2009; published 11 Nov 2009

tuning that may shift the wavelength of one mode of a given cavity without affecting the others. A near-field optical microscope (NSOM) can be used to achieve this effect. Indeed it has been shown that a NSOM probe can be used to alter the modal properties of passive nanophotonic structures [15–22]. These studies hinted that if the electromagnetic coupling between a near-field probe and a photonic mode can be controlled, this could open new avenues for the design of novel optomechanic photonic devices. In this paper, we study theoretically and experimentally the interaction of near-field probes with the modes of an *active* 2D-PC cavity. In particular, the effect of the probe material on the emission wavelength of an electromagnetic nanosource like a 2D-PC nanolaser is investigated. The use of an active device allows light generation directly in the microcavity with no need of access waveguide. Moreover, the demonstration of laser emission while tuning the cavity with a near-field probe needs to be given. After the description of the 2D-PC microcavity and its electromagnetic modes, we study, theoretically, the effect on the modes of a near-field probe placed in the vicinity of the microcavity. We then present NSOM experimental results obtained with different kinds of probes: a bare silica tip, usually used in NSOM characterization because of its minimal impact on the optical field, and a Si-coated silica tip as a more invasive probe.

2. Structure design and numerical simulation

We consider a linear defect nanocavity [23,24] whose design is shown in Fig. 1. The photonic crystal consists of a triangular array of cylindrical holes (period 420 nm and hole radius 100 nm) patterned on a thin InP slab (thickness 250 nm) positioned on top of a SiO_2 substrate The cavity is formed by introducing a linear defect (omitting 7 holes) into the 2D-PC. This defect is referred to as the LC7 microcavity. The cavity structure is designed so as to obtain several spectrally and spatially distinct modes, around 1.5µm. To achieve reasonably high quality factors, the radiation losses were minimized by engineering the holes positions at both edges of the cavity [1]. In our case, the two holes on either side of the cavity were shifted by 80nm outward. The result is an increase by up to 60 percent of the quality factor compared to unmodified microcavity.

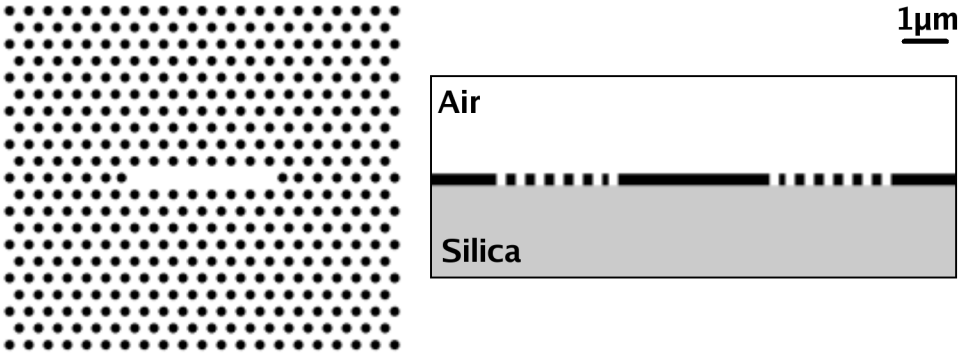

Fig. 1. Views of the calculation domain (a) in the plane of the InP membrane (b) Perpendicular to the InP membrane

The structure was simulated using 3D finite-difference time-domain (FDTD) method with the perfectly matched layers boundary conditions. The full structure lateral size is 11µm x 11µm and consists of the crystal slab on a 2 µm SiO_2 substrate, surrounded by 2 µm of air. Computational meshes were 42 nm for x, y, and z, corresponding to 10 cells for a crystal period. The computations are initially performed without the near-field tip. They show that the microcavity supports several modes, four of them having a quality factor above 1000, the largest found being 5800.

Figure 2.a, 2.b, 2.c and 2.d present the mode cartographies computed at the surface of the InP slab, for the four modes of lowest energy, labeled A (λ = 1444 nm Q = 1615), B (λ = 1483 nm Q = 1000), C (λ = 1517nm Q = 1550) and D (λ = 1530 nm Q = 5800). The fundamental

#116594 - $15.00 USD Received 2 Sep 2009; revised 9 Oct 2009; accepted 9 Oct 2009; published 11 Nov 2009

mode is mode D. The highest quality factor was obtained for this mode which is highly confined into the cavity with the intensity of the mode concentrated principally at the center of the cavity, as it is shown by the vertical cross-section cartography along the longitudinal axis of the cavity (Fig. 2.e). The profile of the central lobe is shown Fig. 2.f. The other modes exhibit a weaker confinement (quality factor around 1000) and different spatial distributions.

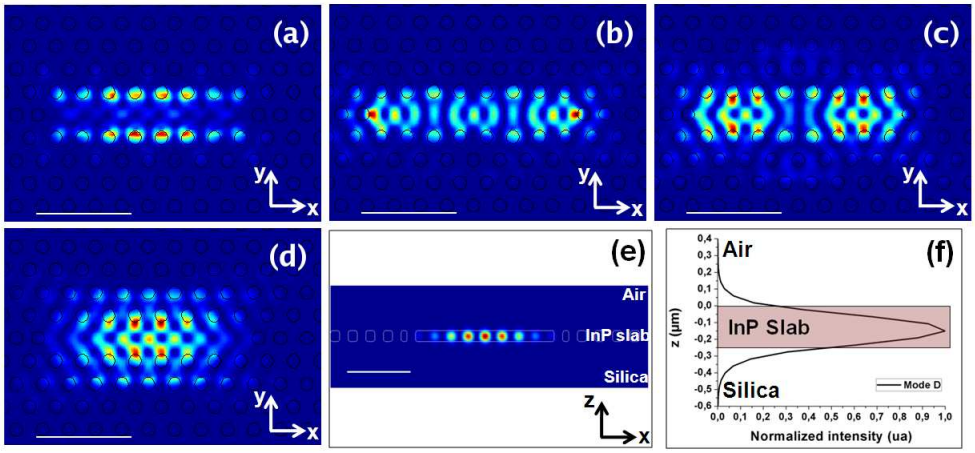

Fig. 2. Horizontal cartography at the surface (z = 0) (a)Mode A: λ = 1444 nm Q = 1615 (b)Mode B: λ = 1483~nm Q = 1000 (c)Mode C: λ = 1517nm Q = 1550 (d)Mode D: λ = 1530~nm Q = 5800 (e) Vertical cross-section cartography of the mode D along the longitudinal axis of the cavity (f) Profile of the central lobe. White bar is 1.5 µm.

This preliminary information about the distribution of light inside the cavity is essential to find which lateral positions of the near-field probe will be most efficient in inducing a change in a given mode. The tip was introduced in the simulation as a truncated cone with an apex radius of 100 nm and an angle of 30°. From the previous simulations, relevant positions corresponding to mode nodes or antinodes can be identified as Pi (i = 0. 1, 2, 3, 4, 5), as shown in Fig. 3. Due to the mesh, the vertical tip position is set 18 nm above the surface. For three positions, namely P2, P4 and P5, the tip is above a hole and the vertical position of the tip can be reduced to 3 nm inside the hole: we defined $P2_{in}$, $P4_{in}$ and $P5_{in}$ as the positions inside the hole and $P2_{out}$, $P4_{out}$, and $P5_{out}$ as the positions above the hole.

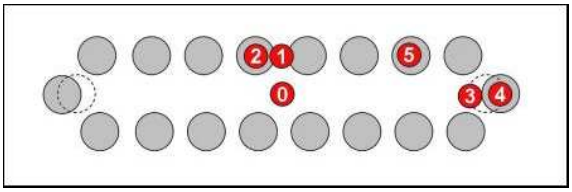

Fig. 3. Simulations have been conducted for different horizontal positions of the tip (18 nm above the cavity): P0, P1, P2, P3, P4 and P5. P2, P4 and P5 include 2 vertical positions, labeled *in* or *out* which are 3 nm inside a hole and 18 nm above a hole, respectively.

We now consider the influence of the near-field probe on the characteristics of the mode D which presents the largest quality factor. Because of its small linewidth, a better visualization of the tip effects is expected for this mode. First, a silica tip (refractive index n = 1.44) is introduced in the computation domain at the positions described previously. Figure 4.a shows that, for mode D, irrespective of the position of the tip, the wavelength shift does not exceed 0.4 nm. The presence of the tip always induces a red shift of the resonance wavelength. It can be easily explained as when the tip penetrates in the near-field of the PC, it contributes to increasing the optical length of the cavity. However, as the refractive index of the silica probe is rather weak, the effect remains moderate. Figure 4.b shows the losses induced by the tip as

#116594 - $15.00 USD Received 2 Sep 2009; revised 9 Oct 2009; accepted 9 Oct 2009; published 11 Nov 2009

a percentage of the losses without tip. It shows that the relative losses induced by the silica tip do not exceed 20% of the initial losses. Though the wavelength of the mode is shifted slightly, these results confirm that an uncoated fiber tip only slightly influences the mode [21] and can, by and large, be considered as a quasi-passive probe. We then conducted similar simulations with a silicon tip. The effects are much more important than for the silica probe. Figure 4.a. shows that, depending on the tip position, the wavelength red-shift can be in the range of 1,5 to 2 nm for tip positions on antinodes. These wavelength shifts are associated with a significant increase in the optical losses (up to 700%, which means that the initial quality factor is divided by 8). Generally, for a given mode a large wavelength shift translates a strong interaction between the probe and the PC, and thus corresponds to large scattering losses. The simulation results also illustrates that the lateral positioning of the tip on a node has less influence than on an antinode, as expected.

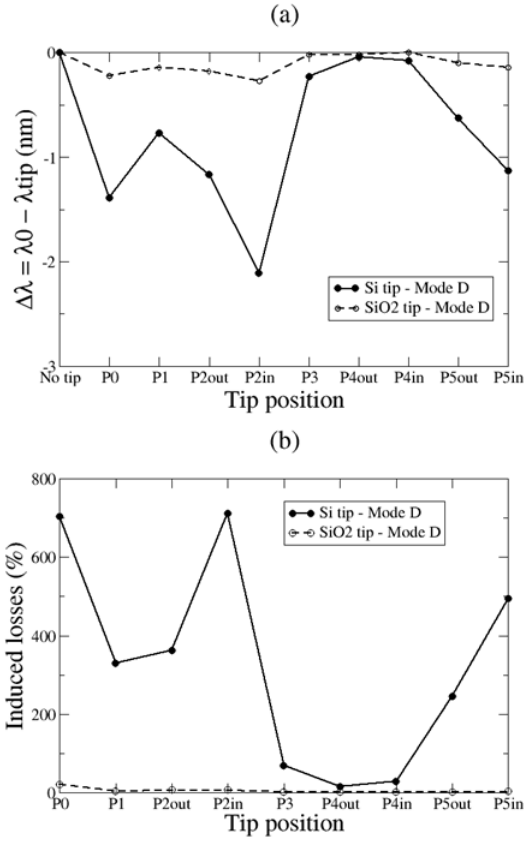

Fig. 4. Evolutions of (a) the resonance wavelength and (b) the relative induced losses depending on silica or silicon tip position obtained by numerical calculations

The silicon tip at position P3 induces the smallest shift (around 0.2 nm with a 70% increase in scattering losses). This is expected as the mode intensity is very weak at P3. The largest shift and the strongest losses are observed when the tip is above an antinode of the mode and penetrates inside a hole of the 2D-PC ($P2_{in}$). Position $P2_{in}$ induces a shift of 2.2 nm with an increase in losses by up to 700%. The relative shift for a lateral translation from position P3 to $P2_{in}$ is 2 nm. The second position with the highest influence is P0 with a relative shift of 1.2 nm from P0 to P3.

#116594 - $15.00 USD Received 2 Sep 2009; revised 9 Oct 2009; accepted 9 Oct 2009; published 11 Nov 2009

3. Experimental configuration

The InP slab is 250 nm thick, has a refractive index of 3.17 at 1.55 µm and supports only one guided mode around that wavelength. Four InAsP quantum wells (QW), separated by InP barrier layers, are grown at the center of the InP slab. The photoluminescence from the QWs occurs between 1250 nm and 1650 nm. This heterostructure is wafer-bonded onto a 1 µm thick SiO_2 layer on top of a silicon host substrate. Compared to photonic crystal cavities fabricated in membranes, this approach yields a better heat sinking and a higher mechanical stability of the structure. The PC is prepared by drilling a triangular lattice of air holes in an InP slab using e-beam lithography and reactive ion etching [25,26]. The NSOM experimental set up has been described in previous work [12,27]. The probe is a chemically etched single mode optical fiber at 1.55µm, with a core diameter of 9µm. The tip apex diameter is around 200 nm with a cone angle of 30°. For the high index tip, the bare silica tip is covered by 50 nm of silicon by e-beam assisted physical vapor deposition. The NSOM is working in collection mode: the tip collects the photoluminescence (PL) in near-field at the surface of the sample. The PC structures are optically pumped at 780 nm with a pulsed laser diode (with a 10% cyclic ratio) and modulated at 2 kHz. The pump beam is focused on the structure with a long work distance objective. Because of the angle of incidence, the pump spot at the surface of the crystal is elliptic with an approximate size of 7µm by 9µm. The photoluminescence signal is collected by the near-field probe and guided to a monochromator (1 nm resolution). A long pass filter is used to eliminate the pump (cutoff wavelength at 1200 nm). The signal is detected with a thermo-electrically cooled InGaAs photodetector. A lock-in amplifier is used to demodulate the signal and enhance the signal to noise ratio. The fiber is attached to a piezoelectric tuning fork setup which allows a shear-force feedback loop to regulate the distance between the tip and the sample (typically between 5 and 15 nm). In this configuration, topographic and photoluminescence images are recorded simultaneously.

4. Results and discussion

The sample was first characterized with the bare silica probe. Figure 5.a and Fig. 5.c show topographies of two LC7 cavities with different parameters: respectively structure X (a = 458 nm and ff = 0.28) and structure Y (a = 460 nm and ff = 0.29) that have similar structure parameters. On those figures, the cavities and the holes of the 2D-PC are clearly visible. Figure 5b and Fig. 5.d show the mode D recorded at 1576 nm for the structure X and 1584 nm for the structure Y. Laser emission is achieved with both modes. The wavelength difference can be explained by non-discerned defects in the structure parameters. We note that in both cases the resolution of the optical map is about λ/6. The near-field maps show a spatial pattern similar to the numerical simulation of mode D. A study over 20 structures shows that if parameter variations due to fabrication modify the resonant wavelength, they do not perturb the spatial distribution of the mode and the laser emission achievement. For each structure the mode D cartography are well reproducible as illustrated on Fig. 5.b and 5.d. Cavity X was chosen to study the influence of the tip.

Figure 6 shows two local near-field spectra recorded on cavity X for two positions of the silica tip: P0 and P3. Depending on the tip position, the local spectrum is different. Mode B (at 1531.5 nm) is clearly detected when the tip is at the position P0 and less visible when the tip is at the position P3. Inversely, mode C (at 1565 nm) is detected at P3 and slightly visible when the tip is at P0.

#116594 - $15.00 USD Received 2 Sep 2009; revised 9 Oct 2009; accepted 9 Oct 2009; published 11 Nov 2009

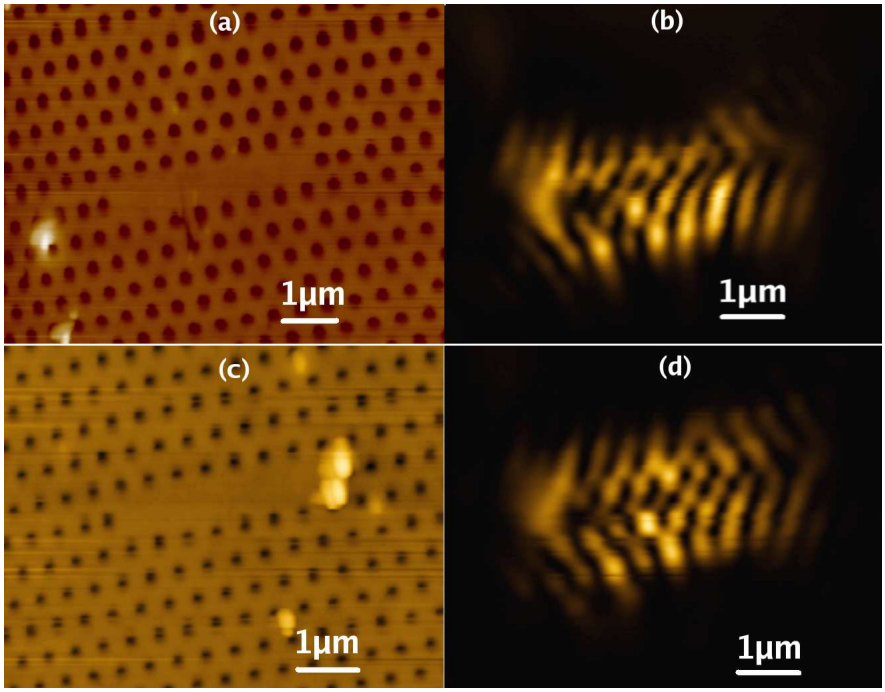

Fig. 5. NSOM characterization with a silica tip of two structures (X and Y) with different parameters: structure X (a = 460 nm r = 112 nm) (a) topography and (b) optical signal of mode D at λ = 1576 nm, structure Y (a = 460 nm r = 105 nm) (c) topography and (d) optical signal of mode D at λ = 1584 nm.

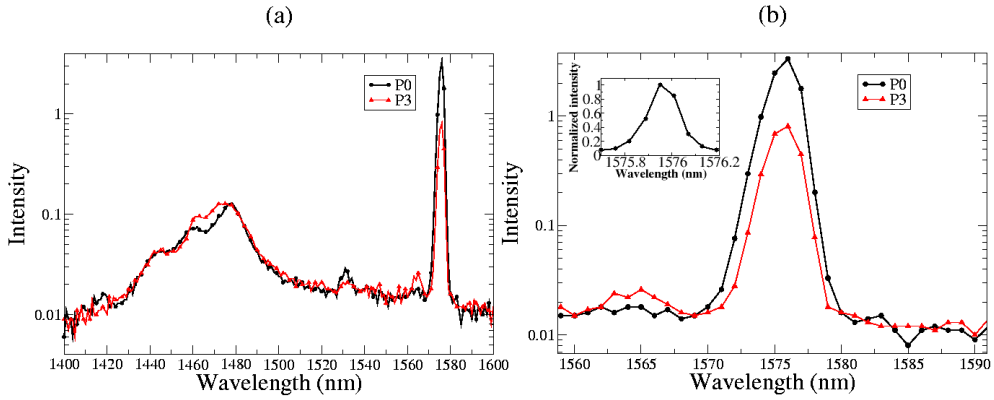

Fig. 6. Influence of NSOM silica tip position on the microcavity resonance wavelength. On the spectra, y axis represents the intensity with a logarithmic scale (a) Near-field spectra above the cavity with several tip position (b) Zoom on the peak at 1576 nm which has the highest intensity

The spectra of Fig. 6.b. show that the intensity of the mode D in P0 is 40 times higher than in P3. No wavelength shift is detected by our set up. The laser peak at Full Width at Half Maximum (FWHM) is 2 nm limited by the resolution of the NSOM set-up. Prior to NSOM measurements, the intrinsic linewidth of the wavelength laser peaks were measured with a far-field refractive optical setup and estimated to be less than 0.2 nm (Inset Fig. 6.b). If a shift is induced by the silica tip, calculations showed that it should be in the range of the intrinsic linewidth of the laser peak, which is beyond the resolution of our set-up. The silica tips may shift slightly the resonance wavelength but the effect is moderate, for the range of the

#116594 - $15.00 USD Received 2 Sep 2009; revised 9 Oct 2009; accepted 9 Oct 2009; published 11 Nov 2009

linewidth of the laser peak. Because the impact of the silica tip is weak, this type of probes is acceptable to quasi-passive characterization [12,27].

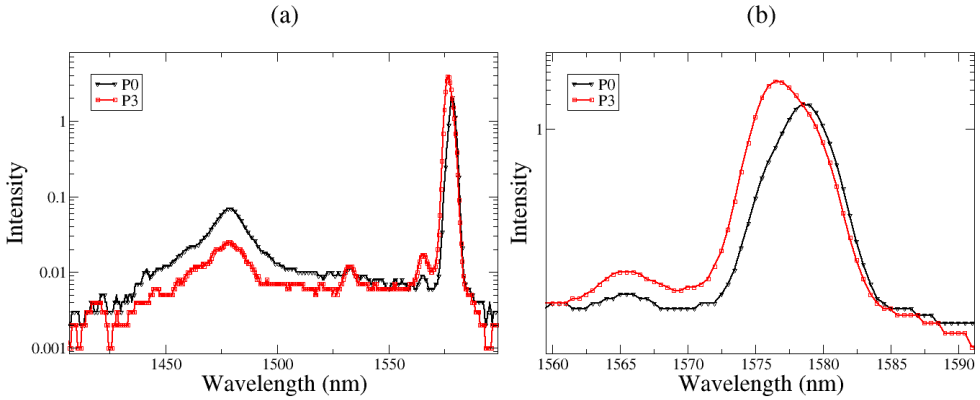

Fig. 7. Influence of NSOM Si-coated tip position on the microcavity resonance wavelength. On the spectra, y axis represents the intensity with a logarithmic scale (a) Near-field spectra above the cavity with several tip position (b) Zoom on the peak at 1578 nm which has the highest intensity

NSOM characterizations were made on the same structure (X) with a high refractive index probe, i.e. a silica probe coated by 50 nm of silicon. Figure 7 shows near-field spectra above the cavity at the previous tip positions: P0 and P3. Because laser emission is still achieved, the FWHM is limited, as before, by the resolution of the NSOM set-up. As expected, the mode D is sensitive to the tip position: a wavelength shift as far as 2 nm is observed depending on the tip position (Fig. 6.b). The resonance is tuned from 1576.5 nm to 1578.5 nm between P3 and P0. This shift is ten times higher than the intrinsic linewidth of the mode. As predicted by the simulations, the position P0 induces a highest wavelength shift than P3, however this value is in agreement with the theoretical prediction.

5. Conclusion

To conclude, the effect of bare silica and Si-coated silica probes on an active 2D-PC structure was investigated. On the one hand, the silica tip induces wavelength shifts in the range of 0.1 nm, which was not detected by our set-up. The impact of the probe, though not negligible, is weak which is still compatible with a passive characterization, especially for low quality factor modes with linewidth in the range of few nanometers. On the other hand, the silicon-coated tip induces a shift in the range of a few nanometers, from 5 to 10 times higher than the intrinsic linewidth of the peak. These theoretical and experimental results illustrate the potential of this concept for the reversible tuning of the wavelength of an active photonic device like a microlaser. In the future, this concept could be exploited to control the efficiency of quantum photonic devices including single QDs and photonic nanocavities.

Acknowledgments

We thank Philippe Regreny for growing the epitaxial structures. The wafer bonding technology was performed at CEA-LETI. We acknowledge the technological support at NANOLYON facility. This work was funded by the French Research National Agency, through the PNANO “ACI Chabip” and “PNANO NANOEC” projects.

#116594 - $15.00 USD Received 2 Sep 2009; revised 9 Oct 2009; accepted 9 Oct 2009; published 11 Nov 2009